Catalysis Science & Technology

Accepted Manuscript

ROYAL SOCIETY OF CHEMISTRY

www.rsc.org/catalysis

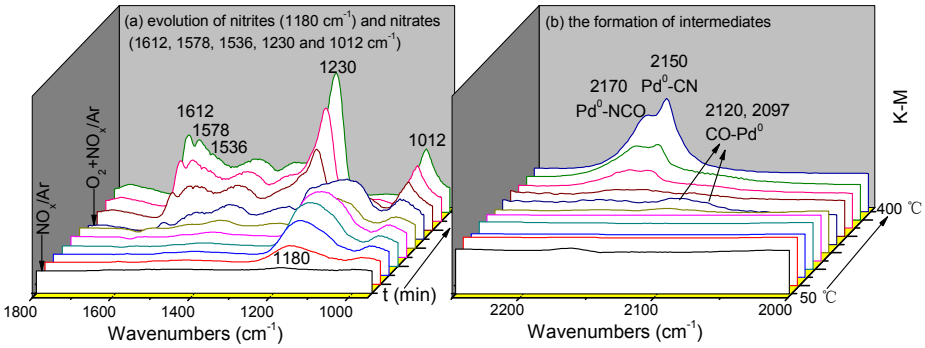

The doping with Ba, especially when the content is 5 wt.%, accelerates the dissociation of NO_x and facilitates the formation of intermediates due to the outstanding electron-donating ability of Ba.

Journal Name

RSCPublishing

ARTICLE

Insights into the role of structural promoter (Ba) in three-way catalyst Pd/CeO_2-ZrO_2 using in situ DRIFTS

Cite this: DOI: 10.1039/xoxxoooooox

Received ooth January 2012,
Accepted ooth January 2012

DOI: 10.1039/xoxxoooooox

www.rsc.org/

Linyan Yang[a], Xue Yang[a], Siyu Lin[a] and Renxian Zhou*[a],

A series of Pd/CeO_2-ZrO_2 (Pd/CZ) catalysts modified with barium oxide with different content were prepared and characterized by XRD, BET, XPS, H_2-TPR and NO_x adsorption/desorption-MS. In particular, the effect of structural promoter (Ba) on the catalytic and surface behaviour was investigated by means of in situ DRIFTS. Doped Ba enters into the CeO_2 lattice, and thus results in the formation of more homogenous Ce-Zr-Ba ternary solid solution, which enhances the textural/structural thermostability and NO_x storage efficiency of the catalysts. DRIFTS results indicate that the introduction of Ba weakens the strong adsorption of HC reactants on the surface of catalysts. Furthermore, the addition of Ba accelerates the dissociation of NO and facilitates the formation of intermediates (NCO and CN) due to the outstanding electron-donating ability of Ba. Therefore, the Ba modified catalysts present much higher catalytic activity of HC and NO_x conversions compared with Pd/CZ. However, the addition of Ba inhibits the oxidation of CO at low temperature resulting from the decreased amount of active sites. In addition, the NO_x operation window is widened with increasing Ba content due to the enhanced NO_x storage capacity.

1. Introduction

Three-way catalysts (TWCs) have been widely used to control automotive exhaust emissions, and catalytic conversion has been proven to be a well-established technology to the abatement of CO, HC and NO_x (NO and NO_2) simultaneously in a narrow window near the stoichiometric air-to-fuel (A/F) ratio[1-3]. Classical components of TWCs usually include Rh, Pt and/or Pd as active metals, ceria-zirconia solid solution (CZ) as promoter for its outstanding oxygen storage ability (OSC)[4-6]. In recent years, CeO_2-ZrO_2-supported Pd-only catalysts have been studied with great interest because of the low cost and high catalytic activity for HC oxidation[7, 8]. However, Pd-only systems have a limitation for the reduction of NO_x[9]. It is well known that the increasingly stringent environmental regulations inevitably demand better efficacy, in particular for the eliminations of HC and NO_x. On the other hand, the catalytic converter is usually located in positions closer to the engine to promote the cold-start performance, and thus the bed temperature of TWCs can rise to even above 1000 ^oC. The serious sintering of TWCs leads to the decline of catalytic activity[10]. Therefore, further improvement in the catalytic performance is of great technological importance.

TWCs usually operate in dynamic mode due to the oscillations in the A/F ratio around the stoichiometric value[3]. The excessive oxygen molecules would seriously inhibit the reduction of NO_x and, hence, many works focused on the improvement of OSC of the supports have been reported[11-13]. Nevertheless, some literatures[14, 15] have reported that the catalytic performance of NO_x reduction under oxygen-rich condition could also be improved by enhancing the NO_x storage capacity. For instance, the introduction of alkaline earth (especially Ba) metals as structural promoter or NO_x absorber has received more attention lately, considering the higher basicity or the electron-donating ability compared with rare earth and transition earth metals[8, 16, 17]. In our previous work[18], we found that the incorporation of alkaline earth metals (such as Ca, Sr and Ba) into CeO_2-ZrO_2 significantly decreased the light-off temperature of NO_x and HC and improved the thermostability of the corresponding catalysts. Furthermore, the NO_x operating window could also be widened due to the improved NO_x storage capacity, especially for the Ba modified catalyst.

Generally, Ce-rich compositions are preferred for the purposes of catalysis and better results are obtained based on $Ce_xZr_{1-x}O_2$ with x ranging from 0.6 to 0.8[19, 20]. To gain further insight into the role of Ba doping in the promoting the catalytic performance, a series of Pd/$Ce_{0.67}Zr_{0.33}O_2$ catalysts modified with BaO with different content were prepared. The textural/structural properties, reducibility and the NO_x storage

ability were characterized by XRD, BET, XPS, H_2-TPR and NO_x adsorption/desorption-MS. In particular, the influence of Ba oxide doping on the formation and reactivity of surface intermediates was investigated by means of in situ DRIFTS.

2. Experimental section

2. 1. Catalysts preparation

A series of $Ce_{0.67}Zr_{0.33}O_2$ supports doped with BaO with different content (3, 5 and 9 wt. %) were prepared through a co-precipitation and supercritical drying method. The mixed solution of ammonia and ammonium carbonate (1.5 mol/L) which was used as precipitator and the quantitative mixed aqueous of precursors ($Ba(NO_3)_2$, $Ce(NO_3)_3 \cdot 6H_2O$, and $ZrO(NO_3)_2 \cdot nH_2O$) were added dropwise to the reactor simultaneously under continuous stirring to maintain the pH at about 9.0. The obtained precipitate was aged at room temperature for 12 h, and then supercritical dried in the medium of ethanol (265 ^oC, >7.0 Mpa) for 2 h. The samples were calcined at 600 ^oC in air for 4 h to obtain supports. The corresponding supported Pd-only catalysts with Pd content of 1.0 wt. % were prepared by conventional wet impregnation method with an aqueous H_2PdCl_4 as metal precursor[18], and the catalysts calcined at 600 ^oC in air for 2 h were named as Pd/CZBx (x=3, 5 and 9). In order to investigate the thermal stability property, all the samples were calcined at 1100 ^oC in air for 4 h, and the corresponding aged catalysts were labeled as Pd/CZBx-a.

2. 2. Catalytic performance studies

Catalytic activity tests were carried out with a fixed-bed continuous flow reactor. The reaction mixture contained 0.745 % O_2, 0.067 % C_3H_6, 0.033 % C_3H_8, 0.75 % CO, 0.1 % NO, 0.03 % NO_2 and balance Ar was fed to the reactor at a GHSV of 43, 000 h^{-1}. The concentrations of CO, NO, NO_2 and total HC (C_3H_6 and C_3H_8) were quantified by an on-line Bruker EQ55 FTIR spectrometer. λ is defined as ($2\nu O_2 + \nu NO + 2\nu NO_2$) / ($\nu CO + 9\nu C_3H_6 + 10\nu C_3H_8$) (ν means concentration in volume percent unit), and the tests of air/fuel operation window were accomplished at different λ values at 400 ^oC[11].

2. 3. Characterization techniques

XPS tests were carried out by a Thermo ESCALAB 250 system with Al Kα radiation (1486.6 eV), operating at 150 W and with energy pass of 20 eV. The binding energies were calibrated by the carbon deposit C 1s binding energy at 284.8 eV.

NO_x adsorption/desorption-MS was conducted in a micro-reactor equipped with mass spectrometer apparatus (Hiden QIC-20). Individual m/z profiles were determined from their relative contribution to the fragments m/z = 30 (NO^+) amu. The catalysts were pretreated at 450 ^oC for 0.5 h under 20 % O_2/Ar flow gas and were subsequently exposed to the reaction gas (0.1 % NO-0.03 % NO_2-0.745 % O_2, Ar balance) at 100 ^oC for 0.5 h. Then, the samples were heated up to 600 ^oC (10 ^oC/min) in high purified Ar stream.

Dispersion of Pd species was calculated on the basis of CO chemisorption using CHEMBET-3000 (Quantachrome Co.). The catalyst (0.2 g) was reduced by purified H_2 at 400 ^oC for 1 h, then purged at 400 ^oC by He for 0.5 h and cooled down to 30 ^oC. CO was pulsed into the sample bed every 5 min until no consumption of CO could be detected.

In addition, the characterization techniques related to N_2-adsorption/desorption, XRD and H_2-TPR were also carried out according to the methods reported in literature[18].

2. 4. In situ DRIFTS measurements

DRIFT spectra were collected using a Nicolet 6700 FTIR with a MCT detector. All spectra were obtained with resolution of 4 cm^{-1} and accumulation of 32 scans. The samples were in situ pretreated for 0.5 h in Ar (10 ml/min) stream at 450 ^oC. Subsequently, the system was cooled down to 30 ^oC in Ar and the background spectra were recorded. Three types of DRIFT experiments were performed: (1) NO_x adsorption experiments were performed at 30 ^oC with a flow of NO_x (0.1 % NO-0.03 % NO_2, Ar balance) for 30 min, and consequently the gas of O_2 was injected into the reactor. The time-resolved spectra of NO_x adsorption were record. (2) CO adsorption experiments were performed at 30 ^oC with a flow of 0.75 % CO/Ar. Prior to CO adsorption, the catalyst was first reduced by purified H_2 at 350 ^oC for 0.5 h and then purged by Ar for 0.5 h. (3) DRIFTS reaction experiments corresponding to simulated reaction mixture were conducted, and spectra were recorded as a function of temperature. The gas concentration and space velocity of the mixture gas were same as the catalytic activity tests.

3. Results and discussion

3. 1. Three-way catalytic performance

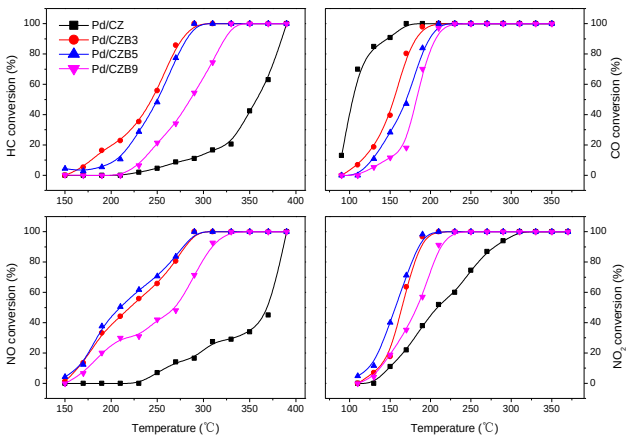

Fig. 1 Light-off curves of HC, CO, NO and NO_2 over the fresh catalysts.

Fig. 1 presents the conversions of HC, CO, NO and NO_2 as a function of temperature under stoichiometric CO+HC+NO_x+O_2 reaction conditions over the fresh catalysts. From Fig. 1, it can be seen that the introduction of Ba significantly promotes the

catalytic activity of HC, NO and NO_2 conversions, as revealed by the decrease of light-off and full-conversion temperature. Among the catalysts tested here, Pd/CZB3 exhibits the best catalytic activity of HC elimination, and the catalytic activity decreases with further increasing Ba content. However, the introduction of Ba seriously inhibits the oxidation of CO considering that the light-off temperature of CO increases with increasing the doping content of Ba. For NO and NO_2 conversions, an improvement is observed with increasing Ba doping content from 3 wt. % to 5 wt. %, whereas a decline is obtained by further increasing the doping content to 9 wt. % (Pd/CZB5 > Pd/CZB3 > Pd/CZB9 > Pd/CZ), signifying that the catalytic activity of NO_x over Pd/CZB5 catalyst is the highest among all the fresh catalysts.

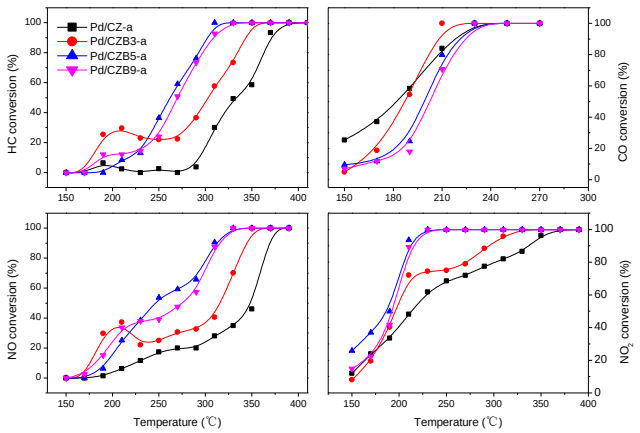

Fig. 2 Light-off curves of HC, CO, NO and NO_2 over aged catalysts.

After thermal aging treatment (Fig. 2), Pd/CZB5-a catalyst exhibits the best catalytic activity for HC and NO_x eliminations, and the catalytic activity decreases in the sequence of Pd/CZB5-a > Pd/CZB9-a > Pd/CZB3-a > Pd/CZ-a. Furthermore, there is no obvious difference in the CO oxidation activity for the catalysts before and after Ba is doped. The above results demonstrate that the addition of Ba is beneficial to promote the thermal aging resistance of the corresponding catalysts.

In this work, the conversions of HC, CO and NO_x under different air/fuel ratios (λ=0.90-1.15) at 400 °C were also tested. The left side of the theoretical stoichiometric value (λ= 1.0) is lean oxygen, and the right is rich oxygen. As shown in Fig. 3A, the conversion of CO reaches 100% under λ ≥ 1 condition but descends with decreasing λ value under λ < 1.0 condition, and the catalytic activity of CO oxidation follows the sequence of Pd/CZB5 > Pd/CZB3 > Pd/CZB9 > Pd/CZ. The conversion of HC over all the Ba modified catalysts reaches 100 % in the test range of λ, whereas the oscillation can be observed over Pd/CZ under λ > 1 condition. Moreover, the catalytic activity of NO_x reduction under λ > 1 condition is significantly promoted with increasing Ba content. The width of the operation window (*W*: λ value width) when CO, HC and NO_x conversions all reach to 90 % under rich and lean conditions follows the sequence of Pd/CZB5> Pd/CZB9 > Pd/CZB3 > Pd/CZ (as listed in Table 1).

The above observations indicate that the introduction of Ba obviously widens the operation window, especially for the eliminations of HC and NO_x under lean-burn condition. After thermal aging treatment (Fig. 3B), the Ba modified catalysts, especially Pd/CZB5-a, still exhibit wider operation window of CO, HC and NO_x conversions compared with Pd/CZ-a.

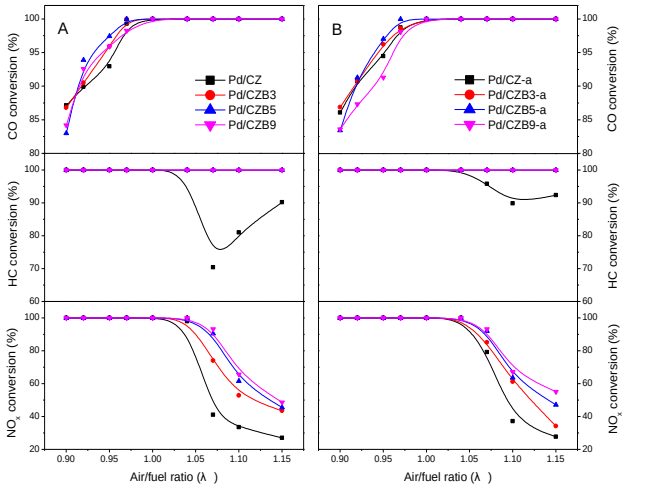

Fig. 3 Conversion curves of CO, HC and NO_x as a function of air/fuel ratio (λ) over the fresh (A) and aged (B) catalysts at 400 °C.

3. 2. Characterization results

3. 2. 1 Textural and structural properties

Table 1 Structural and textural properties of the fresh and aged catalysts

Sample	S_{BET} (m^2/g)	Lattice parameter (Å)	Crystallite size (nm)	*W*
Pd/CZ	46.2	5.4141	8.2	0.11
Pd/CZB3	52.0	5.4243	6.3	0.13
Pd/CZB5	69.8	5.4250	4.8	0.15
Pd/CZB9	61.9	5.4257	5.3	0.16
Pd/CZ-a	7.3	5.4028	29.5	0.13
Pd/CZB3-a	7.1	5.3550	21.1	0.14
Pd/CZB5-a	9.8	5.4011	12.3	0.15
Pd/CZB9-a	8.0	5.3789	19.4	0.13

To gain insight into the role of Ba doping in promoting the catalytic performance of HC and NO_x conversions, the physicochemical properties of the catalysts were investigated in the following sections. As shown in Fig. S1 (supplemental data), all the fresh catalysts with mesoporous structure exhibit wide pore size distribution (2-65 nm), which may be due to the formation of accumulative pore[21]. Moreover, the introduction of Ba increases the specific surface area (Table 1) of the catalysts as a result of improved thermal stability. After aging treatment, a clear decrease in surface area is observed, and the mesoporous structure is also damaged resulting from the severe sintering.

From the XRD patterns as depicted in Fig. 4, it can be seen that the fresh catalysts show broad and symmetric diffraction peaks, with a cubic fluorite structure of CeO_2. The weak diffraction peaks of $BaCO_3$ are detected when the content of Ba is higher than 5 wt. %. This observation indicates that (1) the doped Ba with appropriate content may enter into CZ lattice to

form Ce-Zr-Ba ternary solid solution[10]; (2) the excess Ba species which do not enter into CeO_2 lattice exist mainly in the form of $BaCO_3$. The lattice parameters (Table 1) for the Ba modified catalysts are larger than that of Pd/CZ. One possible explanation is that the ionic radius of Ba^{2+} (1.42 Å) is larger than Zr^{4+} (0.84 Å) and Ce^{3+}/Ce^{4+} (1.14 and 0.97 Å) for eight-coordination. Incorporation of Ba^{2+} into the CZ lattice by substituting Ce^{4+}/Ce^{3+} or Zr^{4+} leads to lattice expansion[22, 23]. Furthermore, the crystallite size obviously decreases with increasing Ba content to 5 wt. %, which confirms the promoted thermal stability arising from the formation of more homogenous solid solution[24].

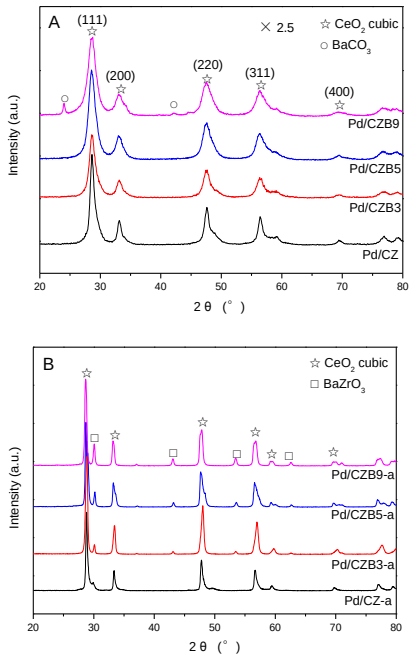

Fig. 4 XRD patterns of the fresh (A) and aged (B) catalysts.

Fig. 4B shows that the peaks become sharper and more intense after aging treatment, corresponding to an increase in the crystalline particle caused by extensive sintering. $BaZrO_3$ phase with orthorhombic structure is observed for Pd/CZBx-a catalysts, and the intensity of the diffraction peak of $BaZrO_3$ increases with increasing Ba content. It can be conclude that, during aging treatment, a portion of Zr^{4+} ions have been extracted from the lattice and coordinated with Ba^{2+} to form $BaZrO_3$. As shown in Table 1, Pd/CZBx-a catalysts present smaller crystallite size, most likely because the formation of $BaZrO_3$ crystallites on oxide particles baffles the agglomeration and restrain the sintering process[4]. In addition, the lattice distortion at the interface of $BaZrO_3/CeO_2$-ZrO_2 mixed oxides could facilitate the formation of oxygen vacancy and increase the mobility of active oxygen atoms at the interface, which may have a positive influence on the catalytic activity of HC and NO_x conversions[18, 25].

3. 2. 2. XPS results

As shown in Fig. 5A, the BE value of Pd $3d_{5/2}$ in Pd/CZ is 337.6 eV corresponding to PdO state, while the peak shifts to lower BE side for Pd/CZBx catalysts. The most possible explanation is that electron density around Pd^{2+} increases due to the electron donation from doped Ba species[26]. Moreover, the peak intensity of Zr 3p decreases with increasing Ba content and the Ce/Zr ratio increases in the sequence of Pd/CZB9 > Pd/CZB5 > Pd/CZB3 > Pd/CZ, indicating that more Zr^{4+} ions are substituted by Ba^{2+}, as evidenced by the decreased surface content of Zr listed in Table 2. From Fig. 5B, it can be seen that the peak intensity of Ba 3d increases with increasing Ba content, and the surface contents of Ba (Table 2) for CZB3 and CZB5 are obviously lower than theoretical values (1.03 and 1.72 at. %). This result also suggests that the doped Ba with appropriate content enters into CZ lattice to form homogenous solid solution.

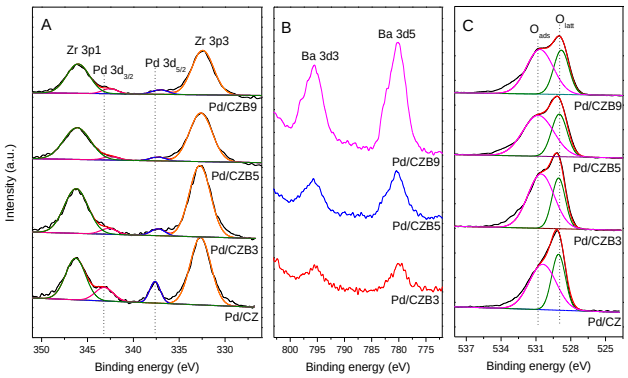

Fig. 5 Zr 3p, Pd 3d (A), Ba 3d (B) and O 1s (C) XPS spectra of the catalysts.

Table 2 Surface elemental composition and atomic ratio measured by XPS

Sample	Surface composition (at. %)				Ce/Zr	Ce^{3+}
	Ce 3d	Zr 3d	Ba 3d	Pd 3d		$3d_{5/2}$ in Ce (%)
Pd/CZ	21.4	7.82	0	0.52	2.74	16.9
Pd/CZB3	21.4	7.38	0.67	0.21	2.90	19.6
Pd/CZB5	23.1	6.06	1.33	0.12	3.81	20.7
Pd/CZB9	22.8	5.12	3.22	0.15	4.45	17.5

As presented in Fig. 5C, the chemisorbed oxygen (O_{ads}) is coexist with lattice oxygen (O_{latt})[4] and relatively lower O_{latt} contents are observed on the Ba doped catalysts. This phenomenon to some extent indicates the higher abundance of oxygen vacancies, which are created to maintain the charge equilibrium after Ba doping. In addition, the concentrations of Ce^{3+} in total Ce for Pd/CZBx catalysts (especially Pd/CZB5) are higher than that of Pd/CZ, demonstrating that the introduction of Ba could promote the transformation from Ce^{4+} to Ce^{3+}. It is generally recognized that the presence of Ce^{3+} is associated with the formation of oxygen vacancy[10].

3. 2. 3. H_2-TPR results

The reducibility is an important factor influencing the three-way catalytic performance and H_2-TPR is a conventional way to investigate the reducibility of the catalysts[27]. For the fresh catalysts (Fig. 6A), the dominant peak α at about 50 °C is ascribed to the reduction of PdO species finely dispersed on the

catalyst surface. The introduction of Ba promotes the reducibility as revealed by the lower reduction temperature, especially for Pd/CZB5. However, the spillover of hydrogen from Pd to the support leads to the reduction of interfacial Ce^{4+}, and thus the amount of H_2 consumption for peak α (508-671 μmol/gcat) over the catalysts is too large to be reasonably attributed to the reduction of PdO species considering that the theoretical amount of H_2 consumption is 94 μmol/gcat, which means that there is a strong interaction between PdO and supports[28].

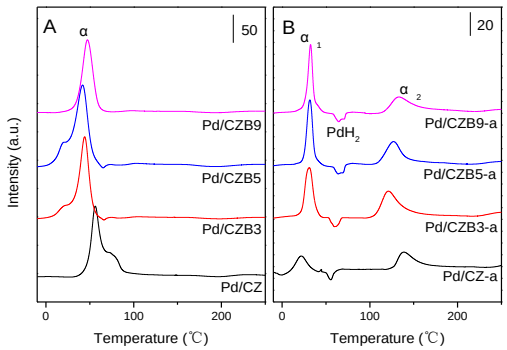

Fig. 6 H_2-TPR traces for the fresh (A) and aged (B) catalysts.

As shown in Fig. 6B, significant changes in the reduction features happen after aging treatment. The negative peak at about 60 °C attributed to the decomposition of PdH_4 species can be observed, because of the formation of large palladium particles[29]. Meanwhile, the peak α splits into two peaks (α_1 and α_2) and obviously decreases in intensity due to the sintering of Pd species. The peak α_1 is assigned to the reduction of PdO species dispersed on the catalyst surface, while the peak α_2 may be related to the reduction of embedded PdO species in CZ support[18]. The introduction of Ba obviously increases the intensity of peak α_1 and lowers the temperature of peak α_2, indicating that the thermal stability of the catalysts are enhanced by the doping of Ba.

3. 2. 4. NO_x adsorption/desorption results

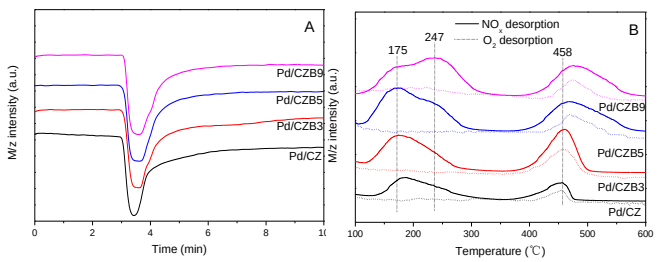

Fig. 7 Adsorption (A) and desorption (B) profiles of NO_x over the catalysts.

The NO_x storage capacity and desorption behaviour were investigated by means of NO_x adsorption/desorption-MS. As presented in Fig. 7A, the addition of Ba obviously enhances the NO_x storage capacity as revealed by the widened NO_x adsorption peak. From Fig. 7B, it can be seen that two broad NO_x desorption peaks appear at the interval of 100-600 °C, meaning the presence of several different NO_x species in a variety of configurations[30]. But the intensities of NO_x desorption peaks obviously increase with increasing Ba content as a result of enhanced NO_x storage capacity. Meanwhile, O_2 species are also tracked during TPD process and the O_2 desorption peak is observed only at around 450 °C. This result indicates that the desorption peak of NO_x observed below 300 °C is mostly related to the decomposition of the instable nitrate species via the evolution of NO, NO_2 and to a lesser extent N_2O and N_2[31], while the desorption peak observed above 400 °C is correlated with the decomposition of stable nitrates as $NO+O_2$[32]. Compared with Pd/CZ, the peak at 247 °C obviously increases in intensity and the peak above 400 °C shifts to higher temperature as the Ba content increases, meaning that the addition of Ba enhances the thermostability of the adsorbed nitrates.

3. 3. In situ DRIFTS results

3. 3. 1. NO_x adsorption

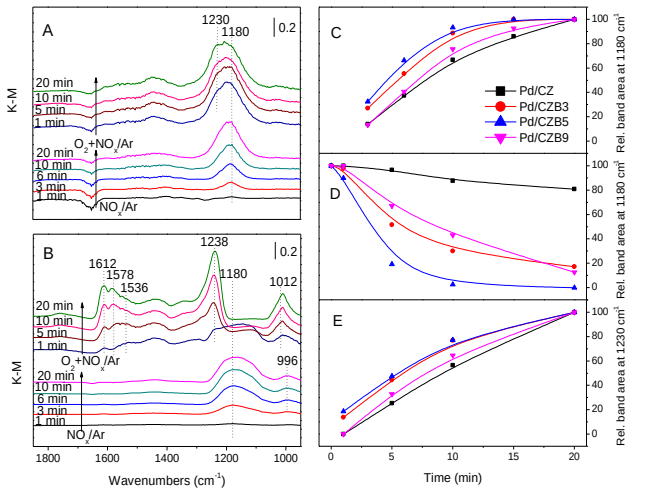

Fig. 8 Time-resolved DRIFT spectra of NO_x adsorption over Pd/CZ (A) and Pd/CZB5 (B), and evolution of nitrites/nitrates with time measured as relative area of 1180 and 1230 cm^{-1} bands under NO_x/Ar (C) and NO_x+O_2/Ar (D and E) flow gas.

To describe the general chemical processes relevant to the adsorption of NO_x over the catalysts and the influence of Ba doping, the time-course DRIFT spectra of NO_x adsorption are presented in Fig. 8A and B. Upon the catalysts exposed to NO_x/Ar gas, the intensities of the bands at 1180 and 996 cm^{-1} assigned to nitrite species gradually increase as a function of time[18, 32]. One possible way for the formation of nitrites is via electron transfer from reduced Ce^{3+} centers to NO_2 molecules to give bonded NO_2^- species, and the Ce^{3+} cations are oxidized to Ce^{4+} with O atoms healing the oxygen vacancies[33]. After stoichiometric O_2 is injected into the NO_x/Ar gas, the bands related to nitrites significantly decrease in intensity, especially over Pd/CZB5. Meanwhile, the intensity of the bands at 1612, 1578, 1536, 1234 and 1010 cm^{-1} ascribed to nitrates in a variety of structures/configurations obviously increases[30, 34, 35]. This phenomenon means that the adsorbed nitrites are oxidized to

nitrates by activated O^* species generated from the adsorption of O_2 following electron transfer by one-electron or two-electron surface defects[32, 33]. Therefore, the formation rate of nitrites and nitrates is donated by electron and oxygen mobility.

The most intense bands related to nitrites and nitrates lie at 1180 and 1230 cm^{-1}, respectively. We therefore consider these two bands as a measure for the rate of nitrites and nitrates formation. Fig. 8C, D and E show the evolution of these species over all the catalysts expressed by the relative band area centred at 1180 and 1230 cm^{-1} as a function of time. It can be seen that the introduction of Ba especially when the content of Ba is 5 wt. % obviously increases the formation rate of nitrites and accelerates the oxidation of nitrites to nitrates, which facilities the storage and elimination of NO_x. As stated in XPS results, the addition of Ba increases the concentration of Ce^{3+} and oxygen vacancies, which promotes the electron and activated oxygen mobility, leading to the higher NO_x storage efficiency over Pd/CZBx[18, 31].

3. 3. 2. CO adsorption

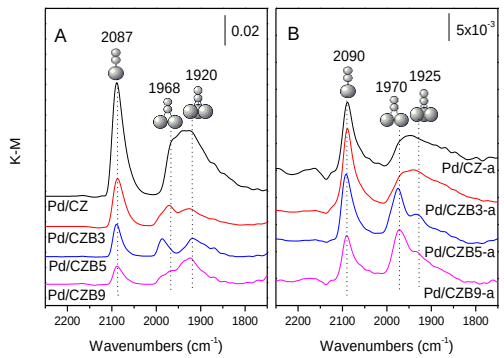

Fig. 9 DRIFTS spectra of CO adsorption over the fresh (A) and aged (B) catalysts.

As the adsorption of CO on metallic palladium sites has different forms, which is depend on the configuration of palladium sites, the in situ CO chemisorption experiments were also performed by using the catalyst with the reduction pretreatment at 30 °C. As shown in Fig. 9, three bands at around 2087, 1968 and 1920 cm^{-1} can be observed. The band at 2090 cm^{-1} is related to the on-top bonded CO molecules on metallic Pd species, whereas the bands at 1968 and 1920 cm^{-1} are assigned to the carbonyls chemisorbed on the bridging and hollow sites of metallic Pd species, respectively[29, 36]. The relative intensities of these bands over the fresh catalysts gradually decrease with increasing Ba content, suggesting that there are less carbonyls adsorbed on active sites for Pd/CZBx due to the obviously decreased dispersion of Pd species (Pd/CZ (40.7 %) > Pd/CZB3 (10.3 %) > Pd/CZB5 (9.1 %) > Pd/CZB9 (6.9 %)). Considering the structurally insensitive character of the CO-O_2 reaction over the supported Pd catalysts, the small structural differences between the Pd particles are not reflected in strong kinetic changes for CO oxidation[3]. Hence, the introduction of Ba inhibits the oxidation of CO due to the reduced amount of active sites on the catalyst surface.

After aging treatment, the intensity of bands related to carbonyls adsorbed on Pd^0 seriously decrease, especially over Pd/CZ-a, due to the reduction in dispersion of Pd species. While the introduction of Ba increases the dispersion in the sequence of Pd/CZB3-a (5.6 %) > Pd/CZB5-a (4.2 %) > Pd/CZB9-a (3.7 %) > Pd/CZ-a (2.0 %), revealing that the modification with Ba improves the thermal aging resistance of the corresponding catalysts and thus inhibits the sintering of active component.

3. 3. 3. In situ DRIFTS results under simulated reaction condition

In order to explore the influence of Ba doping on the formation and reactivity of surface intermediates, detailed DRIFTS studies under the simulated reaction condition have been carried out. As shown in Fig. 10 (DRIFTS spectra over Pd/CZB3 and Pd/CZB9 are shown in Fig. S2, supplementary data), the intensity of the bands at 2930 and 2850 cm^{-1} assigned to the stretching vibrations of hydrocarbon species[37] obviously gets weak with the addition of Ba, demonstrating that the introduction of Ba suppresses the strong adsorption of hydrocarbon species on the catalyst surface and facilitates the catalytic oxidation of HC species.

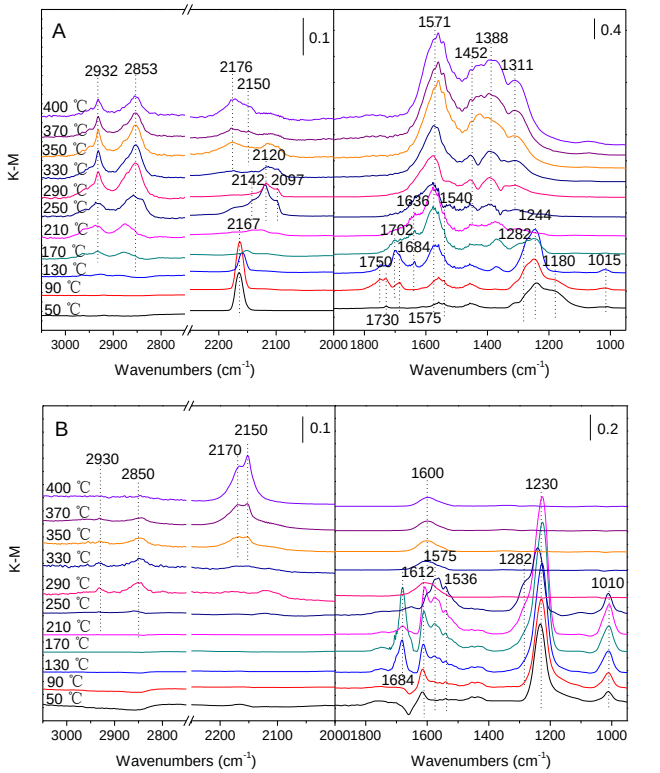

Fig. 10 *In situ* DRIFTS spectra over Pd/CZ (A) and Pd/CZB5 (B) catalysts under simulated reaction condition.

Bands in the region of 2250-2000 cm^{-1} correspond to carbonyls and intermediate species (-NCO and -CN) adsorbed on active metal sites. In these spectra, the band at 2167 cm^{-1} related to CO-Pd^{2+} species[18] can be observed at 50 °C, but decreases in intensity and vanishes with increasing temperature to 170 °C due to the continuous decrease in CO coverage and progressive reduction of PdO species[38]. When the temperature

rises up to 230 °C, bands at 2142 (CO-$Pd^{\delta+}$), 2120 (CO-Pd^{+}) and 2097 cm^{-1} (CO-Pd^{0}) attributed to carbonyls chemisorbed on PdO_x sites are observed[36, 39]. According to the results of catalytic activity test (Fig. 1), the oxidation activity of HC is significantly improved at this temperature, which means that the carbonyls arise from the partial oxidation of HC reactants. Compared with Pd/CZ, the intensity of these bands related to carbonyls are much lower over the Ba modified catalysts, especially over Pd/CZB5, indicating that the addition of Ba, especially when the Ba content is 5 wt. %, facilitates the deep oxidation of HC and thus results in less carbonyls accumulated on the active sites.

When reaction temperature further increases to 350 °C, new bands at around 2172 and 2150 cm^{-1} assigned to isocyanate (NCO) and cyanide (CN) species adsorbed on Pd^0 sites[35] appear, and the band gradually develops with increasing reaction temperature to 400 °C. These NCO and CN species are formed by the interaction of adsorbed N atoms (N^*) with unreacted CO and C^*. In the case of N^* formation which requires the dissociation of NO molecular, two reaction mechanisms have been proposed[40]. The first one involves the unimolecular dissociative adsorption of NO to form N^* and O^*, followed by a rapid removal of O^* by CO or HC to form CO_2. The second one involves a direct bimolecular reaction between NO and CO to form N^* and CO_2. Therefore, the formation of NCO and CN species is usually regarded as a useful fingerprint for monitoring the NO dissociation process. However, compared with Pd/CZ, the intensities of the NCO and CN bands are much stronger over the Ba doped catalysts, especially over Pd/CZB5, indicating that the modification with Ba promotes the formation of intermediate species. It is worth noting that the band related to NCO species shifts to lower wavenumbers with increasing Ba content, which results from the increased electron density of Pd species due to the outstanding electron-donating ability of Ba[2] as stated in XPS results.

Moreover, in the region of 1800-1650 cm^{-1}, bands assigned to NO species adsorbed on metallic Pd sites can be observed. For Pd/CZ, the bands at 1750, 1730 and 1702 cm^{-1} correspond to the linear Pd^0-N=O adsorbed on Pd(112), (111) and (110) facets, respectively[41], while the band at 1684 cm^{-1} is associated to the bent Pd-N=$O^{\delta-}$ species. The active oxygen accumulated around Pd could lower the extent of electron-back-donation into the molecular anti-bonding π^* of NO, and thus results in the formation of Pd-N=$O^{\delta-}$ species[42]. However, compared with Pd/CZ, only the band at 1684 cm^{-1} with much higher intensity can be observed over Ba modified catalysts resulting from the increased electron density of Pd. The dissociation of NO species on Pd sites is strongly structure-sensitive, and the dissociation of the negatively charged Pd-N=$O^{\delta-}$ are more easily compared with neutral Pd-N=O species[42]. Therefore, the modification with Ba facilities the dissociation adsorption of NO and formation of active intermediates, and thus promotes the NO_x reduction activity.

In addition, bands in the range of 1650-950 cm^{-1} can be assigned to nitrite, nitrate and carboxylate species adsorbed on the supports[2]. The band at 1180 cm^{-1} associated with nitrite species is only observed over Pd/CZ below 130 °C, indicating that the introduction of Ba promotes the oxidation of nitrites to nitrates. Above 210 °C, the bands at 1612, 1575, 1540, 1282, 1235 and 1010 cm^{-1} related to nitrates in a variety of structures/configurations vanish, revealing the elimination of nitrates. It is important to note that these bands over Pd/CZBx disappear at higher temperature with increasing Ba content, which may be related to the improved NO_x storage capacity and thermostability as revealed by the NO_x adsorption/desorption-MS results. Moreover, some new bands attributed to carbonates (1571, 1452 and 1311 cm^{-1}), bicarbonate (1636 and 1388 cm^{-1}) and formate species (1600 cm^{-1}) appear at 250 °C and gradually develop with increasing temperature, especially over Pd/CZ. This phenomenon means that, because of the promoted deep oxidation activity of HC species, the introduction of Ba could prevent the poisoning arising from strong adsorption of carboxylate species on the catalyst surface.

Conclusions

A series of Pd/CeO_2-ZrO_2 catalysts doped with Ba with different content (3, 5 and 9 wt. %) were prepared. The role of Ba doping in promoting the catalytic activity of HC and NOx conversions has been investigated by XRD, BET, XPS, H_2-TPR, NO_x adsorption/desorption-MS and in situ DRIFTS. The doped Ba with appropriate content could enter into CeO_2 lattice, leading to the formation of more homogenous Ce-Zr-Ba ternary solid solution, which enhances the textual/structural thermostability. Moreover, the reducibility of the corresponding catalysts was also enhanced, especially when the content of Ba is 5 wt. %. It is important to note that the doping of Ba facilitates the reduction of Ce^{4+} to Ce^{3+} and the formation of oxygen vacancy, which enhances the electron and active oxygen mobility, leading to higher NO_x storage efficiency for the Ba modified catalysts. On the other hand, the modification with Ba facilitates the dissociation adsorption of NO and the formation of intermediates (NCO and CN) due to the outstanding electron-donating ability of Ba. Therefore, Pd/CZBx catalysts exhibit much higher catalytic activity of NO_x reduction and wider NO_x operation window under lean-burn condition compared with Pd/CZ. Furthermore, the doping of Ba weakens the strong adsorption and promotes the deep oxidation activity of HC reactants as revealed by the DRIFTS results. However, the appearance of Ba inhibits the oxidation of CO due to the decreased amount of active sites on the catalyst surface. After thermal aging treatment, the modified catalysts, especially Pd/CZB5-a, still present improved catalytic activity of HC and NO_x conversions due to the enhanced thermostability.

Acknowledgements

We gratefully acknowledge the financial supports from the National Nature Science Foundation of China (No.: 21477109).

Notes and references

[a] Institute of Catalysis, Zhejiang University, Hangzhou 310028, China
Electronic Supplementary Information (ESI) available: the BJH pore size distribution of fresh and aged catalysts, and the in situ DRIFTS spectra over Pd/CZB3 and Pd/CZB9 catalysts under simulated reaction condition. See DOI: 10.1039/b000000x/

[1] M. Konsolakis and I. V. Yentekakis, *Top. Catal.,* 2013, **56**, 165.
[2] V. Matsouka, M. Konsolakis, R. M. Lambert and I. V. Yentekakis, *Appl. Catal. B: Environ.*, 2008, **84**, 715.
[3] A. Mart ínez-Arias, *J. Catal.*, 2004, **221**, 85.
[4] J. Fan, D. Weng, X. D. Wu, X. D. Wu and R. Ran, *J. Catal.*, 2008, **258**, 177.
[5] N. Guill én-Hurtado, A. Bueno-L ópez and A. Garc á-Garc á, *J. Mater. Sci.* 2011, **47**, 3204.
[6] Q. Y. Wang, G. F. Li, B. Zhao and R. X. Zhou, *J. Mol. Catal. A: Chem.*, 2011, **339**, 52.
[7] A. Papavasiliou, A. Tsetsekou, V. Matsouka, M. Konsolakis, I. V. Yentekakis and N. Boukos, *Appl. Catal. B: Environ.*, 2011, **106**, 228.
[8] K. Tanikawa and C. Egawa, *J. Mol. Catal. A: Chem.*, 2011, **349**, 94.
[9] M. Fernández-García, A. Iglesias-Juez, A. Martínez-Arias, A. B. Hungría, J. A. Anderson, J. C. Conesa and J. Soria, *J. Catal.*, 2004, **221**, 594.
[10] Q. Y. Wang, G. F. Li, B. Zhao and R. X. Zhou, *Appl. Catal. B: Environ.*, 2010, **100**, 516-528.
[11] Q. Y. Wang, G. F. Li, B. Zhao, M. Q. Shen and R. X. Zhou, *Appl. Catal. B: Environ.*, 2010, **101**, 150.
[12] Q. Y. Wang, B. Zhao, G. F. Li and R. X. Zhou, *Environ. Sci. Technol.*, 2010, **44**, 3870.
[13] G. F. Li, Q. Y. Wang, B. Zhao and R. X. Zhou, *J. Mol. Catal. A: Chem.*, 2010, **326**, 69.
[14] L. F. Liotta, A. Macaluso, G. E. Arena, M. Livi, G. Centi and G. Deganello, *Catal. Today*, 2002, **75**, 439.
[15] N. A. Ottinger, T. J. Toops, N. Ke, B. G. Bunting and J. Howe, *Appl. Catal. B: Environ.*, 2011, **101**, 486.
[16] M. Yang, Y. Li, J. Wang and M. Shen, *J. Catal.*, 2010, **271**, 228.
[17] E. C. Corbos, S. Elbouazzaoui, X. Courtois, N. Bion, P. Marecot and D. Duprez, *Top. Catal.*, 2007, **42-43**, 9.
[18] L. Y. Yang, S. Y. Lin, X. Yang, W. M. Fang and R. X. Zhou, *J. Hazard. Mater.*, 2014, **279**, 226.
[19] D. Terribile, A. Trovarelli, J. Llorca, C. de Leitenburg and G. Dolcetti, *Catal. Today*, 1998, **43**, 79.
[20] M. Boaro, C. Leitenburg, G. Dolcetti and A. Trovarelli, *J. Catal.*, 2000, **193**, 338.
[21] G. F. Li, Q. Y. Wang, B. Zhao and R. X. Zhou, *Catal. Today*, 2011, **175**, 40.
[22] Y. Q. Jia, *J. solid state che*m., 1991, **95**, 184.
[23] R. D. Shannon, *Acta Crystallogr.*, 1967. **A32**. 751.
[24] G. Li, B. Zhao, Q. Wang and R. Zhou, *Appl. Catal. B: Environ.*, 2010, **97**, 41.
[25] E. Mamontov, R. Brezny, M. Koranne and T. Egami, *J. Phys. Chem. B*, 2003, **107**, 13007.
[26] T. Kobayashi, T. Yamada, K. Kayano, *Appl. Catal. B: Environ.*, 2001, **30**, 287.
[27] S. Salasc, V. Perrichon, M. Primet and N. Mouaddib-Moral, *J. Catal.*, 2002, **206**, 82.
[28] Q. Y. Wang, G. F. Li, B. Zhao and R. X. Zhou, *J. Hazard. Mater.*, 2011, **189**, 150.
[29] S. Lin, L. Yang, X. Yang and R. Zhou, *Appl. Surf. Sci.*, 2014, **305**, 642.
[30] S. Roy, N. van Vegten, N. Maeda and A. Baiker, *Appl. Catal. B: Environ.*, 2012, **119-120**, 279.
[31] B. Azambre, L. Zenboury, A. Koch and J. V. Weber, *J. Phys. Chem. C*, 2009, **113**, 13287.
[32] I. Atribak, B. Azambre, A. Bueno L ópez and A. Garc á-Garc á, *Appl. Catal. B: Environ.*, 2009, **92**, 126.
[33] B. Azambre, I. Atribak, A. Bueno-Lopez and A. Garcia-Garcia, *J. Phys. Chem. C*, 2010, **114**, 13300.
[34] T. Baidya, P. Bera, B. D. Mukri, S. K. Parida, O. Kr öcher, M. Elsener and M. S. Hegde, *J. Catal.*, 2013, **303**, 117.
[35] A. Martinez-Arias, M. Fernandez-Garcia, A. B. Hungria, A. Iglesias-Juez, K. Duncan, R. Smith, J. A. Anderson, J. C. Conesa and J. Soria, *J. Catal.*, 2001, **204**, 238.
[36] K. Zorn, S. Giorgio, E. Halwax, C. R. Henry, H. Gronbeck and G. Rupprechter, *J. Phys. Chem. C*, 2011, **115**, 1103.
[37] V. Matsouka, M. Konsolakis, I. V. Yentekakis, A. Papavasiliou, A. Tsetsekou and N. Boukos, *Top. Catal.*, 2011, **54**, 1124.
[38] M. Fernández-García, A. Martínez-Arias, A. Iglesias-Juez, A. B. Hungría, J. A. Anderson, J. C. Conesa and J. Soria, *J. Catal.*, 2003, **214**, 220.
[39] O. S. Alexeev, S. Krishnamoorthy, C. Jensen, M. S. Ziebarth, G. Yaluris, T. G. Roberie and M. D. Amiridis, *Catal. Today*, 2007, **127**, 189.
[40] S. K. Matam, M. A. Newton, A. Weidenkaff and D. Ferri, *Catal. Today*, 2013, **205**, 3.
[41] K. Almusaiteer and S. S. C. Chuang, *J. Catal.*, 1998, **180**, 161.
[42] P. Granger, C. Dujardin, J. F. Paul and G. Leclercq, *J. Mol. Catal. A: Chem.*, 2005, **228**, 241.

